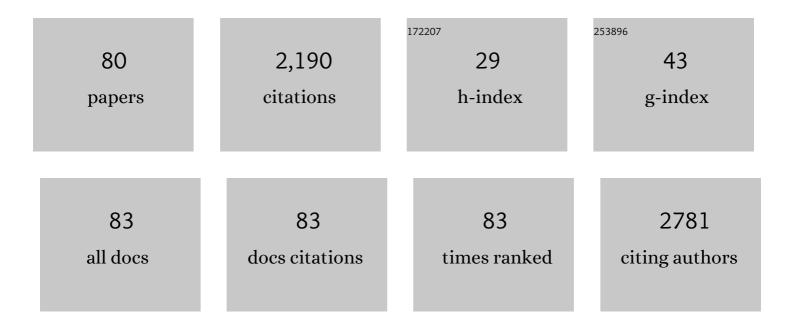
Chung-Yul Yoo

List of Publications by Year in descending order

Source: https://exaly.com/author-pdf/6786064/publications.pdf Version: 2024-02-01



#	Article	IF	CITATIONS
1	Flow-electrode capacitive deionization with highly enhanced salt removal performance utilizing high-aspect ratio functionalized carbon nanotubes. Water Research, 2019, 151, 252-259.	5.3	116
2	Communication—Electrochemical Reduction of Nitrogen to Ammonia in 2-Propanol under Ambient Temperature and Pressure. Journal of the Electrochemical Society, 2016, 163, F610-F612.	1.3	109
3	Ultrafast charge transfer coupled with lattice phonons in two-dimensional covalent organic frameworks. Nature Communications, 2019, 10, 1873.	5.8	93
4	Electrochemical Synthesis of Ammonia from Water and Nitrogen in Ethylenediamine under Ambient Temperature and Pressure. Journal of the Electrochemical Society, 2016, 163, F1523-F1526.	1.3	81
5	Electrochemical ammonia synthesis from steam and nitrogen using proton conducting yttrium doped barium zirconate electrolyte with silver, platinum, and lanthanum strontium cobalt ferrite electrocatalyst. Journal of Power Sources, 2015, 284, 245-251.	4.0	78
6	Electrochemical Synthesis of Ammonia from Water and Nitrogen: A Lithiumâ€Mediated Approach Using Lithiumâ€ion Conducting Glass Ceramics. ChemSusChem, 2018, 11, 120-124.	3.6	71
7	Performance and stability of niobium-substituted Ba0.5Sr0.5Co0.8Fe0.2O3â~δ membranes. Solid State Ionics, 2011, 195, 1-6.	1.3	69
8	Phase transformation and oxygen equilibration kinetics of pure and Zr-doped Ba0.5Sr0.5Co0.8Fe0.2O3â^î´ perovskite oxide probed by electrical conductivity relaxation. Applied Physics Letters, 2010, 96, .	1.5	68
9	5L-Scale Magnesio-Milling Reduction of Nanostructured SiO ₂ for High Capacity Silicon Anodes in Lithium-Ion Batteries. Nano Letters, 2016, 16, 7261-7269.	4.5	67
10	Pseudocapacitive slurry electrodes using redox-active quinone for high-performance flow capacitors: an atomic-level understanding of pore texture and capacitance enhancement. Journal of Materials Chemistry A, 2015, 3, 23323-23332.	5.2	58
11	Dramatically Enhanced Oxygen Fluxes in Fluorite-Rich Dual-Phase Membrane by Surface Modification. Chemistry of Materials, 2014, 26, 4387-4394.	3.2	52
12	Precisely Geometry Controlled Microsupercapacitors for Ultrahigh Areal Capacitance, Volumetric Capacitance, and Energy Density. Chemistry of Materials, 2018, 30, 3979-3990.	3.2	52
13	Electrochemical analysis of slurry electrodes for flow-electrode capacitive deionization. Journal of Electroanalytical Chemistry, 2017, 806, 50-60.	1.9	51
14	Oxygen surface exchange kinetics of SrTi1â^xFexO3â^î^ mixed conducting oxides. Physical Chemistry Chemical Physics, 2012, 14, 11759.	1.3	46
15	Contribution of the surface exchange kinetics to the oxygen transport properties in Gd0.1Ce0.9O2â^Îr–La0.6Sr0.4Co0.2Fe0.8O3â^Î^dual-phase membrane. Solid State Ionics, 2013, 253, 64-69.	1.3	45
16	High-Power-Density Skutterudite-Based Thermoelectric Modules with Ultralow Contact Resistivity Using Fe–Ni Metallization Layers. ACS Applied Energy Materials, 2018, 1, 1603-1611.	2.5	44
17	The effects of NiO addition on the structure and transport properties of proton conducting BaZr0.8Y0.2O3â°'. Journal of Alloys and Compounds, 2015, 621, 263-267.	2.8	43
18	Investigation of Lithium Ion Diffusion of Graphite Anode by the Galvanostatic Intermittent Titration Technique. Materials, 2021, 14, 4683.	1.3	43

#	Article	IF	CITATIONS
19	Bulk transport and oxygen surface exchange of the mixed ionic–electronic conductor Ce1â^'xTbxO2â^'Î′ (x = 0.1, 0.2, 0.5). Journal of Materials Chemistry A, 2013, 1, 10234.	5.2	40
20	Electrochemical Ammonia Synthesis Mediated by Titanocene Dichloride in Aqueous Electrolytes under Ambient Conditions. ACS Sustainable Chemistry and Engineering, 2017, 5, 9662-9666.	3.2	40
21	Oxygen transport kinetics of the misfit layered oxide Ca ₃ Co ₄ O _{9+δ} . Journal of Materials Chemistry A, 2014, 2, 19717-19725.	5.2	38
22	Mussel-inspired surface functionalization of porous carbon nanosheets using polydopamine and Fe ³⁺ /tannic acid layers for high-performance electrochemical capacitors. Journal of Materials Chemistry A, 2017, 5, 25368-25377.	5.2	37
23	Oxygen surface exchange kinetics of erbia-stabilized bismuth oxide. Journal of Solid State Electrochemistry, 2011, 15, 231-236.	1.2	36
24	Substantial Oxygen Flux in Dual-Phase Membrane of Ceria and Pure Electronic Conductor by Tailoring the Surface. ACS Applied Materials & Interfaces, 2015, 7, 14699-14707.	4.0	34
25	Chemically and thermo-mechanically stable LSM–YSZ segmented oxygen permeable ceramic membrane. Journal of Membrane Science, 2015, 486, 222-228.	4.1	32
26	Enhanced salt removal performance of flow electrode capacitive deionization with high cell operational potential. Separation and Purification Technology, 2021, 254, 117500.	3.9	32
27	Low-cost and energy-efficient asymmetric nickel electrode for alkaline water electrolysis. International Journal of Hydrogen Energy, 2015, 40, 10720-10725.	3.8	31
28	Electrochemical synthesis of ammonia from water and nitrogen catalyzed by nano-Fe2O3 and CoFe2O4 suspended in a molten LiCl-KCl-CsCl electrolyte. Korean Journal of Chemical Engineering, 2016, 33, 1777-1780.	1.2	31
29	Energy storage and generation through desalination using flow-electrodes capacitive deionization. Journal of Industrial and Engineering Chemistry, 2020, 81, 317-322.	2.9	31
30	Continuous Lithium Extraction from Aqueous Solution Using Flow-Electrode Capacitive Deionization. Energies, 2019, 12, 2913.	1.6	30
31	Self-templated synthesis of interconnected porous carbon nanosheets with controllable pore size: Mechanism and electrochemical capacitor application. Microporous and Mesoporous Materials, 2018, 261, 119-125.	2.2	28
32	Improved Desalination Performance of Flow- and Fixed-Capacitive Deionization using Redox-Active Quinone. ACS Sustainable Chemistry and Engineering, 2020, 8, 16701-16710.	3.2	27
33	Structural and Electrochemical Properties of Dense Yttria-Doped Barium Zirconate Prepared by Solid-State Reactive Sintering. Energies, 2018, 11, 3083.	1.6	26
34	Enhanced Desalination Performance of Capacitive Deionization Using Nanoporous Carbon Derived from ZIF-67 Metal Organic Frameworks and CNTs. Nanomaterials, 2020, 10, 2091.	1.9	24
35	Oxygen surface exchange kinetics on PrBaCo2O5+Ĩ´. Solid State Ionics, 2014, 262, 668-671.	1.3	21
36	Enhanced durability of a proton conducting oxide fuel cell with a purified yttrium-doped barium zirconate-cerate electrolyte. Journal of Power Sources, 2015, 278, 320-324.	4.0	20

#	Article	IF	CITATIONS
37	A new strategy for enhancing the thermo-mechanical and chemical stability of dual-phase mixed ionic electronic conductor oxygen membranes. Journal of Materials Chemistry A, 2016, 4, 13549-13554.	5.2	20
38	Role of Protons in Electrochemical Ammonia Synthesis Using Solid-State Electrolytes. ACS Sustainable Chemistry and Engineering, 2017, 5, 7972-7978.	3.2	20
39	Enhanced chemical stability and sinterability of refined proton-conducting perovskite: Case study of BaCe0.5Zr0.3Y0.2O3â^1´. Journal of the European Ceramic Society, 2015, 35, 1855-1863.	2.8	17
40	Oxidation suppression characteristics of the YSZ coating on Mg 2 Si thermoelectric legs. Ceramics International, 2016, 42, 10279-10288.	2.3	17
41	Effects of Ni diffusion on the accelerated conductivity degradation of scandia-stabilized zirconia films under a reducing atmosphere. Journal of the European Ceramic Society, 2016, 36, 1835-1839.	2.8	17
42	Investigation of Electrochemical Properties of Model Lanthanum Strontium Cobalt Ferrite-Based Cathodes for Proton Ceramic Fuel Cells. Electrocatalysis, 2016, 7, 280-286.	1.5	17
43	Anion-exchange-membrane-based electrochemical synthesis of ammonia as a carrier of hydrogen energy. Korean Journal of Chemical Engineering, 2018, 35, 1620-1625.	1.2	17
44	Unraveling Crystal Structure and Transport Properties of Fast Ion Conducting SrCo _{0.9} Nb _{0.1} O _{3â^Î} . Journal of Physical Chemistry C, 2016, 120, 22248-22256.	1.5	16
45	Determination of oxygen nonstoichiometry in SrFeO _{3â^'Î′} by solidâ€state Coulometric titration. Journal of the American Ceramic Society, 2017, 100, 2690-2699.	1.9	16
46	Impedance spectroscopy for assessment of thermoelectric module properties under a practical operating temperature. Energy, 2018, 152, 834-839.	4.5	16
47	Lithium-Mediated Ammonia Electro-Synthesis: Effect of CsClO ₄ on Lithium Plating Efficiency and Ammonia Synthesis. Journal of the Electrochemical Society, 2018, 165, F1027-F1031.	1.3	16
48	Electrochemical Synthesis of Ammonia from Water and Nitrogen using a Pt/GDC/Pt Cell. Korean Chemical Engineering Research, 2014, 52, 58-62.	0.2	16
49	Electroactive self-polymerized dopamine with improved desalination performance for flow- and fixed- electrodes capacitive deionization. Applied Surface Science, 2022, 579, 152154.	3.1	16
50	The effects of Fe-substitution on the crystal structure and oxygen permeability of PrBaCo2O5+δ. Materials Letters, 2013, 108, 65-68.	1.3	15
51	Novel oxygen transport membranes with tunable segmented structures. Journal of Materials Chemistry A, 2014, 2, 8174-8178.	5.2	15
52	Electrical characteristics and detailed interfacial structures of Ag/Ni metallization on polycrystalline thermoelectric SnSe. Journal of Materials Science and Technology, 2019, 35, 711-718.	5.6	15
53	Ag/Ni Metallization Bilayer: A Functional Layer for Highly Efficient Polycrystalline SnSe Thermoelectric Modules. Journal of Electronic Materials, 2017, 46, 848-855.	1.0	14
54	Chloroaluminate Anion Intercalation in Graphene and Graphite: From Two-Dimensional Devices to Aluminum-Ion Batteries. Nano Letters, 2022, 22, 1726-1733.	4.5	13

#	Article	IF	CITATIONS
55	ZIF-67 metal-organic frameworks and CNTs-derived nanoporous carbon structures as novel electrodes for flow-electrode capacitive deionization. Separation and Purification Technology, 2021, 277, 119466.	3.9	12
56	Attachable micropseudocapacitors using highly swollen laser-induced-graphene electrodes. Chemical Engineering Journal, 2020, 386, 123972.	6.6	11
57	Crucial role of a nickel substrate in Co3O4 pseudocapacitor directly grown on nickel and its electrochemical properties. Journal of Alloys and Compounds, 2016, 676, 407-413.	2.8	10
58	A new layered perovskite, KSrNb ₂ O ₆ F, by powder neutron diffraction. Acta Crystallographica Section C: Crystal Structure Communications, 2007, 63, i63-i65.	0.4	9
59	Dimensional modification of oxyfluoride lattice: Preparation and structure of A′ANb2O6F (A′=Na, K,) Tj ETG	Qq110.7	84314 rgBT
60	Synthesis, crystal structure, and ionic conductivity of a new layered metal phosphate, Li2Sr2Al(PO4)3. Journal of Solid State Chemistry, 2016, 243, 12-17.	1.4	9
61	Preparation of metal oxide/polyaniline/N-MWCNT hybrid composite electrodes for electrocatalytic synthesis of ammonia at atmospheric pressure. Sustainable Energy and Fuels, 2019, 3, 431-438.	2.5	9
62	Determination of the thermoelectric properties of a skutterudite-based device at practical operating temperatures by impedance spectroscopy. Applied Energy, 2019, 251, 113341.	5.1	9
63	Single-crystalline Co2Si nanowires directly synthesized on silicon substrate for high-performance micro-supercapacitor. Chemical Engineering Journal, 2019, 370, 973-979.	6.6	8
64	Thermal diffusion barrier metallization based on Co–Mo powder-mixed composites for n-type skutterudite ((Mm,Sm)yCo4Sb12) thermoelectric devices. Journal of Alloys and Compounds, 2020, 818, 152917.	2.8	8
65	Crystal structures of new layered perovskite-type oxyfluorides, CsANb2O6F (A = Sr and Ca) and comparison with pyrochlore-type CsNb2O5F. Journal of Solid State Chemistry, 2018, 267, 146-152.	1.4	6
66	Univariate and multivariate analyses of Gd in gadolinia-doped ceria using laser-induced breakdown spectroscopy. Optik, 2021, 240, 166909.	1.4	6
67	Preparation, crystal structure, and oxygen permeability of Pr 0.5 Sr 0.5 Co 1â^'x Fe x O 3â^'î´ perovskites. Materials Letters, 2015, 161, 33-36.	1.3	5
68	Oxygen surface exchange kinetics of Ba0.5Sr0.5Co0.8Fe0.2O3â~δ. Physical Chemistry Chemical Physics, 2020, 22, 10158-10169.	1.3	5
69	Quantitative analysis of ceria co-doped with samarium and gadolinium using laser-induced breakdown spectroscopy. Analytical Methods, 2022, , .	1.3	5
70	Practical evaluation of electrical contact resistance of thermoelectric legs at high operation temperature. Journal of Materials Science: Materials in Electronics, 2019, 30, 14112-14119.	1.1	4
71	Comparative Study of Epoxy-CsH2PO4 Composite Electrolytes and Porous Metal Based Electrocatalysts for Solid Acid Electrochemical Cells. Membranes, 2021, 11, 196.	1.4	4
72	Multivariate stoichiometric analysis of gadolinium-doped ceria using low-power low-resolution laser-induced breakdown spectroscopy. Optik, 2021, 247, 167919.	1.4	4

#	Article	IF	CITATIONS
73	KCaNb ₂ O ₆ F from a combined synchrotron X-ray and neutron powder diffraction study. Acta Crystallographica Section E: Structure Reports Online, 2007, 63, i203-i204.	0.2	3
74	Soft chemical synthesis and the role of potassium pentahydrogen bis(phosphate) in a proton conducting composite electrolyte based on potassium dihydrogen phosphate. Journal of Power Sources, 2014, 260, 159-162.	4.0	3
75	Mosaic-shaped cathode for highly durable solid oxide fuel cell under thermal stress. Journal of Power Sources, 2014, 247, 534-538.	4.0	3
76	Effects of Nb and Sn co-doping on the structure and properties of SrCoO _{3-<i>δ</i>} oxygen transport membranes. Journal of Asian Ceramic Societies, 2020, 8, 519-527.	1.0	3
77	Synchrotron study of the garnet-type oxide Li ₆ CaSm ₂ Ta ₂ O ₁₂ . Acta Crystallographica Section E: Structure Reports Online, 2009, 65, i74-i74.	0.2	2
78	Oxidation and sublimation suppression of PbTe thermoelectric legs by plasma coated ceramic layers. Journal of Vacuum Science and Technology A: Vacuum, Surfaces and Films, 2016, 34, 061101.	0.9	2
79	Direct Comparison of Thermoelectric Devices Using Impedance Spectroscopy. Journal of Electronic Materials, 2019, 48, 1833-1839.	1.0	1
80	Oxygen permeation and oxidative coupling of methane with NiFe2O4-Gd0.1Ce0.9O2-l´ composite membrane. Ionics, 2021, 27, 1667-1675.	1.2	1